

Saturated fatty acids and fatty acid esters promotes the polymorphic transition of clarithromycin metastable form I crystal

Miteki Watanabe ^a, Midori Mizoguchi ^a, Hajime Aoki ^a, Yasunori Iwao ^a, Shuji Noguchi ^{a, b}, Shigeru Itai ^{a*}

^a *School of Pharmaceutical Sciences, University of Shizuoka, 52-1 Yada, Suruga-ku, Shizuoka 422-8526, Japan*

^b *Faculty of Pharmaceutical Sciences, Toho University, 2-2-1 Miyama, Funabashi-city, Chiba 274-8510, Japan*

*Corresponding author. E-mail: s-itai@u-shizuoka-ken.ac.jp; Tel.: +81-54-264-5614; Fax: +81-54-264-5615.

Abbreviations: CAM, clarithromycin; GM, glycerin monostearate; LW, Lubliwax-101; TR-FB, triglycerin full behenate; DSC, differential scanning calorimetry; PXRD, powder X-ray diffraction.

Abstract

The phase transition of active pharmaceutical ingredients should be taken into account during manufacturing, processing- and storage, because different crystal forms lead to different physical properties of formulations. The phase transition of clarithromycin (CAM) metastable form I to stable form II was investigated on heating with additives such as fatty acids or fatty acid esters. Differential scanning calorimetry analyses revealed that when form I was heated with additives, the phase transition temperature of form I decreased close to the melting points of the additives. Powder X-ray diffraction analyses indicated the tentative presence of a non-crystalline component during the transition of form I to form II on heating with additives. These observations implied that CAM form I dissolved in the melted additives on heating and the dissolved CAM crystallized to form II. Reduction of transition temperatures in the presence of additives were also observed for the crystals of nifedipine form B and carbamazepine form III. These results suggested that the phenomena can be widely applicable for simultaneous crystalline phase transition and granulation using binder additives.

Key words: Clarithromycin, Crystalline phase transition, Powder-X-ray diffraction, Differential scanning calorimetry, Metastable, Melt granulation

1. Introduction

Clarithromycin (CAM) is a 14-membered macrolide antibiotic with broad-spectrum activity against various bacteria. CAM has been widely used for the clinical treatment of various infectious diseases including the eradication of *Helicobacter pylori*. Eight crystal forms of CAM have been reported: form 0 (ethanol solvate; Spanton et al., 1999), form I (Liu et al., 1999), form II (Tozuka et al., 2002), form III (acetonitrile solvate; Liang and Yao, 2007), form IV (hydrate; Avrutov et al., 2003), form V (Gruss et al., 2008), hydrochloride salts (Parvez et al., 2000; Noguchi et al., 2014), and methanol solvate (Iwasaki et al., 1993). Because different crystal forms lead to different physical properties such as solubility, dissolution rate, compression ability, and bioavailability (Yu et al., 1998; Fujiki et al., 2015), the phase transition of active pharmaceutical ingredients must be taken into account during processing and storage. At present, CAM formulation for medical treatment contains the most stable form II (Liu et al., 1998). However, the manufacture of form II requires significant time and cost because it is prepared by the crystalline phase transition from metastable form I by heating over 140°C (Tozuka et al., 2002).

Recently, the effects of wet granulation on CAM crystal forms were investigated (Nozawa et al., 2015). Phase transition from CAM form I to form II was promoted by wet granulation using water in the presence of polysorbate 80, polyoxyl 40 stearate or macrogol 400, and polymorphic transition from form II to form I during wet granulation using an organic solvent such as ethanol can be prevented by including these additives. This phenomenon makes it possible to manufacture products containing stable form of CAM using organic solvents without contamination of crystalline polymorphs. Phase transition from form I to form II was also reported to be induced by a melt granulation process (Itai et al., 2014). Phase transition from form I to form II was completed during melt granulation at a temperature much lower than 140°C under the presence of low melting binders such as fatty acids and fatty acid esters. These phenomena can be applied to simultaneous

granulation and crystalline phase transition to reduce time and costs for manufacturing granules made from CAM form II. However, their mechanisms are yet to be defined.

In this study, the mechanism responsible for reducing the phase-transition temperature by including additives such as a fatty acid ester or fatty acid was investigated by differential scanning calorimetry (DSC) and powder X-ray diffraction (PXRD). These additives were also investigated for their ability to reduce the phase transition temperatures of other drugs such as the crystals of nifedipine form B and carbamazepine form III.

2. Materials and Methods

2.1. Materials

CAM, nifedipine, and carbamazepine were purchased from Shiono Chemical., Co. Ltd. (Tokyo, Japan), Tokyo Chemical Industry Co., Ltd. (Tokyo, Japan), and Wako Pure Chemical Industries, Ltd. (Osaka, Japan), respectively. Glycerin monostearate (GM) and Gelucire43/01 were purchased from Taiyo Kagaku Co. Ltd. (Mie, Japan), and CBC Co., Ltd (Tokyo, Japan), respectively. Lauric acid, myristic acid, palmitic acid, stearic acid, palmitic anhydride, and stearic anhydride were purchased from Tokyo Chemical Industry Co., Ltd. (Tokyo, Japan). Lubliwax-101(LW) and triglycerin full behenate (TR-FB) were kindly supplied by Freund Corporation (Tokyo, Japan), and RiKen Vitamin Co., Ltd. (Tokyo, Japan), respectively.

2.2. Preparation of CAM form I crystals

CAM form I was prepared by recrystallization of bulk form II from ethanol followed by vacuum drying for 24 h at room temperature. The obtained crystals were milled using a mortar and pestle, and sieved through a 149- μm or a 50- μm mesh. Crystals passed through the 149- μm mesh were used for DSC analysis, and crystals passed through the 50- μm mesh were used for PXRD to minimize the

preferential orientation effect. The crystal form of the CAM form I was confirmed by using the PXRD system (Mini Flex II, Rigaku Corp., Tokyo, Japan).

2.3. Preparation of nifedipine form B crystals and carbamazepine form III crystals

Glassy nifedipine was prepared by heating bulk nifedipine (form A) at 200°C for 10 min, and cooling melted nifedipine down to 0°C. Form B was prepared by milling glassy nifedipine using a mortar and pestle (Chan et al., 2004). Crystal forms of nifedipine form B were analyzed by using the PXRD system.

Purchased carbamazepine crystals were form III as confirmed by PXRD. The crystals were sieved through a 149- μm mesh, and were used for further analyses.

2.4. DSC analyses

CAM form I (0.4 g) and additives (0.1 g) were put into a plastic bag and mixed for 3 min by shaking. Ten milligrams of the mixture was put into an aluminum pan and analyzed by DSC using a DSC7020 (Hitachi High-Tech Science Corp., Tokyo, Japan). The heating rate was 10°C/min and the nitrogen gas flow was 40 mL/min. Nifedipine form B and carbamazepine form III were mixed with GM or stearic acid, and the mixtures were analyzed in a similar fashion as the CAM form I mixtures.

2.5. PXRD analyses

Crystal forms of carbamazepine form III and form III/GM or stearic acid mixtures heated at 100°C for 20 min were analyzed by PXRD using Mini Flex II (Rigaku Corp., Tokyo, Japan).

2.6. PXRD using synchrotron X-ray

CAM form I sieved through 50- μm mesh and an additive were mixed for 3 min in a plastic bag. The

mixing ratio by weight between form I and an additive was 4:1. Form I crystals and Form I/additive mixtures were enclosed into capillaries with diameters of 0.3 mm. PXRD data were collected at the Aichi synchrotron radiation center BL5S2, which is equipped with a Debye-Sherrer camera and Pilatus 100K (Rigaku, Tokyo, Japan). The wavelength was set to 1.000 Å. The diffraction patterns with a 2θ range of 1.86–16.23° were recorded. The samples were heated at 10°C/min with nitrogen gas flow. The exposure time was 18 or 6 s.

The amounts of form I and form II were estimated using the integrated intensities of (1 1 0) reflection ($2\theta = \text{approx. } 6.6^\circ$) and (0 1 1) reflection ($2\theta = \text{approx. } 6.1^\circ$), respectively. Because the observed integrated intensity $y(T)$ showed a sigmoidal shape as a function of temperature T , the following sigmoid equation was fitted to $y(T)$ by a least-squares method to determine the parameters, y_{max} , k , T_h , and A :

$$y(T) = \frac{y_{\text{max}}}{1 + e^{-k(T - T_h)}} + A,$$

where $(y(T) - A)/y_{\text{max}}$ is the amount of the crystal form of interest, and T_h is the temperature where 50% of the crystal form is transitioned or formed. T_h values for form I and form II were defined as T_1 and T_2 . The tangents at T_1 and T_2 , were calculated from the equation $\frac{dy}{dT}(T_h) = ky_{\text{max}}/4$, and their absolute values, a_1 and a_2 , were used to evaluate the rates of the phase transition reaction.

The cell parameters of CAM form I during heating were calculated from the powder diffraction profiles by using EXPO2014 (Altomare et al., 2013).

2.7. Calculation of solubility parameters

The solubility parameters δ of CAM and saturated fatty acids were calculated based on the equation below as the index of solubility of CAM into saturated fatty acids:

$$\delta = \sqrt{\frac{(\Delta H - RT)}{V}},$$

where ΔH is the molar heat of vaporization, R is the gas constant, T is the temperature, and V is the molar volume. V was calculated by division of molar mass M by density ρ ($V = M / \rho$), and the density of the CAM crystal was calculated by using the lattice constant. Moreover, the solubility parameter at 70°C, δ_{70} , was estimated by using the equation below because the solubility parameter becomes inappropriate when the temperature significantly departs from 25°C (Yonezawa et al., 2006).

$$\delta_{70} = \frac{V_{25}}{V_{70}} \times \delta_{25}$$

V_{25} and V_{70} are molar volume at 25°C and 70°C, respectively, and δ_{25} is the solubility parameter at 25°C.

3. Results and Discussion

3.1. Evaluation of the phase transition temperature using DSC analysis

The DSC thermogram of form I showed the exothermic peak around 140°C corresponding to the phase transition from form I to form II, and the endothermic peak around 220°C corresponding to the melting of form II (Fig. 1 (a)). This data was corresponding to the previous data reported by Tozuka et al., (2002). However, the DSC thermograms of the form I/GM mixture did not show the exothermic peak around 140°C corresponding to the phase transition (Fig. 1 (b)), and instead, the exothermic peak appeared around 78°C, slightly higher than the melting point of GM, which is around 73°C. Exothermic peaks corresponding to the phase transition around 140°C also disappeared in DSC thermograms of LW, TR-FB, myristic acid, stearic acid, palmitic acid, palmitic anhydride, stearic anhydride, Gelucire43/01 and lauric acid mixtures, and exothermic peaks were observed at temperatures slightly higher than the melting points (40–80°C) of the additives (Fig. 1 (c)–(k)). All the mixtures showed endothermic peaks around 200–220°C, confirming that form I in the mixtures transformed to form II. These observations indicated that the phase transition

temperatures from form I to form II were reduced to the values closer to the melting points of the additives.

3.2. Quantitative evaluation of the phase transition of CAM form I induced by including additives

3.2.1. CAM form I without additives

PXRD analysis during increasing temperature was carried out to clarify the mechanism responsible for the reduction in phase transition temperature that became obvious by DSC analysis.

When form I without additives was heated, the crystal form remained as form I up to approximately 123°C as shown in Fig. 1(a). However, slight changes in some lattice parameters of CAM form I were observed (Fig. 2). The space group of form I was $P2_12_12$ and the cell parameters at 30°C were $a = 14.46 \text{ \AA}$, $b = 34.77 \text{ \AA}$, and $c = 8.716 \text{ \AA}$. The length of the b -axis increased linearly up to $+0.15 \text{ \AA}$ and the length of the c -axis increased up to $+0.02 \text{ \AA}$, whereas the length of the a -axis was almost constant. In the form I crystal, CAM molecules are aligned in a head-to-tail manner parallel to the a -axis and intermolecular hydrogen bonds were formed only in the head-to-tail molecular alignment (Noguchi et al., 2012). The invariant length of the a -axis might be ascribable to these structural aspects of the form I crystal.

When form I was heated to around 123°C, the diffraction intensities of form I ($2\theta =$ approx. 6.6°) started to decrease and, instead, diffraction peaks of form II ($2\theta =$ approx. 6.1°) appeared and their intensities increased (Fig. 3 (a)). The diffraction intensities of form II reached almost maximum at approximately 155°C. The temperatures at which the form I ratio decreased to 50% and the form II ratio increased to 50%, T_1 and T_2 , were almost same, 141°C and 141°C. The sum of form I and form II was almost 100% throughout this temperature range (Fig. 3 (a), green dot line denotes 100 (%)– (sum of form I and form II (%))), and no diffraction peak other than those of form I and form II was observed. These observations suggested that transformation of form I to form

II proceeded rapidly without a stable intermediate component.

3.2.2. CAM form I / additive mixture

When the form I/GM mixture was heated, the amount of form I started to decrease at about 65°C, and form II started to be produced at about 65°C (Fig. 3 (b)). The phase transition proceeded rapidly as was evident from the fact that T_1 at 70.3°C almost coincided with T_2 at 70.4°C (Table 1). The stable intermediate component that was neither form I nor form II did not exist similar to the case for form I without an additive. A reduction in the phase transition temperature in the absence of the stable intermediate component also occurred when form I was heated with LW, TR-FB, or myristic acid (Fig.3 (c) (d) (e)).

In contrast to these observations, when the form I/stearic acid mixture was heated, form I started to decrease at about 50°C, but form II was not produced around this temperature (Fig. 3 (f)). Form II was produced starting at about 65°C, and finished at about 80°C. During this process, sum of form I and form II was less than 100% and no diffraction peak was observed except those of form I and form II, suggesting that non-crystalline component of CAM was present. The non-crystalline component, amount of which can be calculated by the $100 (\%) - (\text{sum of form I and form II} (\%))$, emerged at about 50°C, reached maximum amount at about 65°C, and then started to decrease. When the form I/palmitic acid, palmitic anhydride, or stearic anhydride mixture was heated, the phase transition temperature of form I decreased and the presence of non-crystalline component was also confirmed (Fig.3 (g) (h) (i)). When form I/Gelucire 43/01 was heated, form I started to decrease at about 40°C and form II and the non-crystalline component started to be produced at the same time (Fig. 3 (j)). The non-crystalline component reached a maximum amount at about 50°C, and then started to decrease. When the form I/lauric acid mixture was heated, form II and the non-crystalline component were produced at the same time as in the case of adding Gelucire43/01 (Fig.3 (k)). The

non-crystalline component might be CAM dissolved into the melted additives because it emerged at the temperature near the melting points of the additives. The non-crystalline component could be scarcely detected when form I was heated with GM, LW, TR-FB or myristic acid (Fig.3 (b) (c) (d) (e)). This might be because the amount of the CAM dissolved in the additives might be very small or form II crystallized rapidly, as was clear from the fact that the differences between T_1 and T_2 were much small, less than 1°C, when form I was heated with more hydrophilic additives, such as GM, LW, or TR-FB (Table 1). In contrast, the polarities of palmitic acid and stearic acid would be low because they have long aliphatic hydrocarbon chains whereas the polarities of GM and LW would be high because they have some hydrophilic hydroxyl moieties. Therefore, the amount of hydrophobic CAM that dissolved in stearic acid or palmitic acid would be high. As a result, it took longer time to reach saturation, resulting in the large differences between T_1 and T_2 . When the form I/stearic acid mixture was heated, T_2 at 70.7°C was much higher, by approximately 7°C, than T_1 at 63.8°C (Fig.3 (f), Table 1); The large differences between T_1 and T_2 were found in the cases for saturated fatty acids or saturated fatty acid anhydrides with low polarities. These might be ascribable to the difference in the solubility of CAM into the melted additives. In the case of myristic acid, the difference of T_1 and T_2 was small for some reason.

The relationship between the temperatures T_1 and T_2 , and the absolute values of the reaction rates calculated from the fitted sigmoid curves, a_1 and a_2 , were plotted as functions of the number of carbon atoms of the saturated fatty acids as shown in Fig. 4. Large a_1 indicated that form I rapidly dissolved in the additive, and large a_2 indicated that form II rapidly crystallized from the dissolved CAM component. As the carbon chain of the saturated fatty acid becomes longer, the melting point of the saturated fatty acid becomes higher, suggesting that T_1 increases in general; nevertheless, T_1 decreased. That was possibly because it was easier for form I to dissolve in the additive as was evident from the fact that a_1 increased. The observed increase in a_1 and decrease in

T_1 probably occurred because the form I solubility into the saturated fatty acids became higher as the fatty acid carbon chain became long. Moreover, a_2 increased and T_2 decreased as the carbon chain of the saturated fatty acid became longer. The observed increase in a_2 and decrease in T_2 probably occurred because form II crystallized more rapidly as the amount of CAM dissolved in the saturated fatty acid increased. We hypothesized that form I dissolves in the additive, and form II crystallizes when the additive becomes supersaturated. These phenomena are possibly caused whichever additive we add to CAM form I.

The relationship between the number of carbon atoms of the saturated fatty acid and the difference in their solubility parameters to that of CAM is shown in Fig. 5. It is known that two components can be easily mixed when the differences between their solubility parameters are small. The solubility parameters of CAM, lauric acid, myristic acid, palmitic acid, stearic acid were 14.0, 15.0, 14.2, 13.3, 12.7 (J/cm^3)^{1/2}, respectively. The differences between the solubility parameters decreased as the saturated fatty acid chain became longer (Fig. 5). This suggested that form I was easily dissolved in the additive as the chain became longer.

3.3. Effect of the amount of additives on the phase transition of CAM form I

PXRD analysis of CAM form I/GM or stearic acid in the stage of phase transition during increasing temperature was carried out when the percentage of GM or stearic acid was changed (Figs. 6 and 7). The phase transition temperatures T_1 and T_2 decreased, and the phase transition rates a_1 and a_2 increased as the percentage of GM added into form I increased (Fig. 6 (a), (b)). This might be because the amount of form I dissolved in GM increased as the percentage of GM increased. This trend was also observed when a saturated fatty acid with a longer carbon chain was added to form I. However, in the case of GM, non-crystalline component did not increase even though the percentage of GM increased (Figs. 3 and 7 (a) (b)). This was possibly because CAM that dissolved in GM is

unstable. As a result, form II crystallized extremely rapidly from CAM dissolved in GM.

In the case of the form I/stearic acid mixture, T_1 decreased but T_2 was not minimum value when 50% stearic acid was added (Fig. 6 (c)). The amount of non-crystalline component increased as the percentage of stearic acid increased, and reached 100% at 60–100°C when 50% stearic acid was added (Fig. 7 (d)). When the percentage of stearic acid increased, the concentration of form I dissolved in stearic acid became lower and the degree of supersaturation decreased. This resulted in higher T_2 , because a longer time was required for the crystal nuclei of form II to be generated. The phase transition rates a_1 and a_2 were increased as the percentage of stearic acid increased as in the case of GM (Fig. 6 (d)).

3.4. Effect of additives on the phase transition temperature of the metastable crystal of nifedipine and carbamazepine

DSC analysis was carried out to determine whether the reduction in phase transition temperature also occurred in other drugs. The drugs nifedipine form B and carbamazepine form III were chosen for the study because they are known to show crystalline polymorphic phase transition.

DSC thermograms of nifedipine form B showed the exothermic peak around 100°C corresponding to the phase transition to form A, a stable form of nifedipine, and the endothermic peak around 176°C corresponding to melting of form A (Hirayama et al., 1994). DSC thermograms of the form B/GM or stearic acid mixture showed the exothermic peak around 80°C which is slightly higher than the melting point of GM, and the disappearance of an exothermic peak around 100°C (Fig. 8 (a)). The endothermic peak corresponding to the melting of form A was evident around 168°C, although melting point of form A was lowered by about 9°C. These indicated that the phase transition temperature of nifedipine could be also lowered by adding additive, possibly by the same mechanism as CAM form I.

DSC thermograms of carbamazepine form III showed the endothermic peak around 156°C

corresponding to melting of form III and recrystallization to form I, and the endothermic peak around 196°C corresponding to melting of form I (Rustichelli et al., 2000). DSC thermograms of the form III/GM showed two endothermic peaks around 100°C and 190°C corresponding to melting point of GM and form I, respectively, while the endothermic peak around 176°C disappeared (Fig. 8 (b)). The transition temperature from form III to form I might be reduced and its endothermic peak might be integrated with the endothermic peak corresponding to the melting of stearic acid around 70°C. Accordingly, crystal forms of carbamazepine form III and form III/GM or stearic acid mixture at 100°C were analyzed by PXRD. Form III heated at 100°C for 20 min remained as it was compared with reference form III (Fig. 9). Form III did not transform to form I at 100°C. However, form III/GM or stearic acid heated at 100°C for 20 min changed into form I compared with the reference form I. Form III transformed to form I at 100°C when heated with additives. Therefore, the temperature of phase transition which involved the melting of crystal could be also lowered by using additives to the drug.

The fact that low-melting point additives could also reduce the phase transition temperatures of metastable crystals other than CAM implied the wide applicability of this method for preparing stable crystal forms of active pharmaceutical ingredients at low cost.

4. Conclusions

In this study, the metastable form I of CAM was shown to transform to stable form II at a lower temperature by using additives such as fatty acids and fatty acid esters. It was suggested that when including additives, form I dissolved in the melted additive, and then form II crystallized from the dissolved non-crystalline component. When saturated fatty acids were used as additives, the phase transition temperature lowered as the hydrocarbon chain of the saturated fatty acid became longer. The phase transition temperature was also lowered as the percentage by weight of the additives

increased. Moreover, the addition of additives to metastable drugs other than CAM resulted in the lowering of the phase transition temperature. Therefore, this suggested that it would be possible to reduce the time and cost of manufacturing a crystal form of a drug that requires heating at a high temperature.

Acknowledgments

The synchrotron radiation experiment at BL5S2 at Aichi SR was performed with the approval of the Aichi Synchrotron Radiation Center, Aichi Science & Technology Foundation, Aichi, Japan (Proposal Nos. 201501002 and 201503006). This work was supported by the Japan Society for the Promotion of Science KAKENHI (Grant Nos. 26460224, 26460039, and 26460226).

References

- Altomare, A., Cuocci, C., Giacobuzzo, C., Moliterni, A., Rizzi, R., Corriero N., Falcicchio A., 2013. EXPO2013: a kit of tools for phasing crystal structures from powder data. *J. Appl. Crystallogr.* 46, 1231–1235.
- Avrutov, I., Lifshitz, I., Borochovit, R., Masarwa, B., Schwartz, E., inventor; Teva Pharmaceutical Industries Ltd., assignee, 2003. Processes for preparing clarithromycin polymorphs and novel polymorph IV. United State patent 6599884. Jul 29.
- Chan, K. L. A., Fleming, O. S., Kazarian, S. G., Vassou, D., Chryssikos, G. D., Gionis, V., 2004. Polymorphism and devitrification of nifedipine under controlled humidity: a combined FT-Raman, IR and Raman microscopic investigation. *J. Raman Spectrosc.* 35, 353–359.
- Fujiki, S., Watanabe, N., Iwao, Y., Noguchi, S., Mizoguchi, M., Iwamura, T., Itai, S., 2015. Suppressed release of clarithromycin from tablets by crystalline phase transition of metastable polymorph form I. *J. Pharm. Sci.* 104, 2641–2644.
- Gruss, M, inventor; Gruenenthal GmbH., assignee, 2008. Polymorph of Clarithromycin (Form V). United State patent 20080249035. Oct 9.
- Hirayama, F., Zheng, W., Uekama, K., 1994. Effect of 2-hydroxypropyl- β -cyclodextrin on crystallization and polymorphic transition of nifedipine in solid state. *Pharm. Res.* 11, 1766–1770.
- Itai, S., Noguchi, S., Iwao, Y., Nozawa, K, Aoki, H., Japanese patent application 2014-197259.
- Iwasaki, H., Sugawara, Y., Adachi, T., Morimoto, S., Watanabe, Y., 1993. Structure of 6-O-methylerythromycin A (clarithromycin). *Acta Crystallogr.* C49, 1227–1230.
- Noguchi, S., Mimura, K., Fujiki, S., Iwao, Y., Itai, S., 2012. Clarithromycin form I determined by synchrotron X-ray powder diffraction. *Acta Crystallogr.* C68, o41–o44

- Noguchi, S., Takiyama, K., Fujiki, S., Iwao, Y., Miura, K., Itai, S., 2014. Polymorphic transformation of antibiotic clarithromycin under acidic condition. *J. Pharm. Sci.* 103, 580–586.
- Nozawa, K., Iwao, Y., Noguchi, S., Itai, S., 2015. Effect of surfactants or a water soluble polymer on the crystal transition of clarithromycin during a wet granulation process. *Int. J. Pharm.* 495, 204–217.
- Liang, J.H., Yao, G.W., 2008. A new crystal structure of clarithromycin. *J. Chem. Crystallogr.* 38, 61–64.
- Liu, J-H., Riley, D.A., inventor; Abbott Laboratories., assignee, 1998. Preparation of crystal form II of clarithromycin. United State patent 5844105. Dec 1.
- Liu, J-H., Riley, D.A., Spanton, S.G., inventor; Abbott Laboratories., assignee, 1999. Crystal form I of clarithromycin. United State patent 5858986. Jan 12.
- Parvez, M., Arayne, M.S., Sabri, R., Sultana, N., 2000. Clarithromycin hydrochloride 3.5-hydrate. *Acta Crystallogr. C*56, 398–399.
- Rustichelli, C., Gamberini, G., Ferioli, V., Gamberini, M.C., Ficarra, R., Tommasini, S., 2000. Solid-state study of polymorphic drug: carbamazepine. *J Pharm Biomed Anal.* 23, 41–54
- Spanton, S.G., Henry, R.F., Riley, D.A., Liu, J-H, inventor; Abbott Laboratories., assignee, 1999. Crystal form O of clarithromycin. United State patent 5945405. Aug 31.
- Tozuka, Y., Ito, A., Seki, H., Oguchi, T., Yamamoto, K., 2002. Characterization and quantitation of clarithromycin polymorphs by powder X-ray diffractometry and solid-state NMR spectroscopy. *Chem. Pharm. Bull* 50, 1128–1130.
- Yonezawa, S., Kobuchi, S., Fukuchi, K., Shimoyama, Y., Arai, Y., 2006. Prediction method of solubility parameter based on molecular structure. *Soc. Master. Eng. Resour. Japan* 19, 25-27

Yu, L., Reutzel, S.M., Stephenson, G.A., 1998. Physical characterization of polymorphic drugs: an integrated characterization strategy. *Pharm. Sci. Technol. Today* 1, 118–127.

Table 1 Effect of the additive agent on the phase transition temperature and transition rate of CAM form I

	T_1 (°C)	T_2 (°C)	a_1 (°C ⁻¹)	a_2 (°C ⁻¹)
GM(5%)	72.2	72.3	0.221	0.156
GM(20%)	70.3	70.4	0.221	0.238
GM(50%)	67.8	68.3	0.259	0.266
LW	79.5	79.7	0.087	0.088
TR-FB	71.0	71.4	0.177	0.163
Gelucire43/01	48.2	52.5	0.072	0.062
Stearic acid(5%)	86.3	91.1	0.019	0.019
Stearic acid(20%)	63.8	70.7	0.055	0.119
Stearic acid(50%)	55.2	108.1	0.102	0.205
Palmitic acid	64.0	74.4	0.038	0.115
Myristic acid	80.0	80.2	0.052	0.050
Lauric acid	71.5	80.3	0.036	0.043
Stearic anhydride	74.5	112.0	0.016	0.038
Palmitic anhydride	82.2	107.5	0.012	0.055

The ratio of LW, TR-FB, Gelucire43/01, palmitic acid, myristic acid, lauric acid, palmitic anhydride, stearic anhydride was 20%.

Figure captions

Fig. 1 DSC thermograms of CAM form I/additive mixture.

(a) Form I, (b) Form I + GM, (c) Form I + LW, (d) Form I + TR-FB, (e) Form I + Myristic acid, (f) Form I + Stearic acid, (g) Form I + Palmitic acid, (h) Form I + Palmitic anhydride, (i) Form I + Stearic anhydride, (j) Form I + Gelucire43/01, (k) Form I + Lauric acid. Solid and dotted lines indicate the DSC profiles of form I + additive and additive only, respectively.

Fig. 2 Changes of lattice constants of form I during the increasing temperature. The lengths of a , b , and c are shown with red circles, purple squares, and green triangles, respectively. Lattice constants at 30°C were $a = 14.46 \text{ \AA}$, $b = 34.77 \text{ \AA}$, and $c = 8.72 \text{ \AA}$.

Fig. 3 Quantitative analysis of form I, form II and amorphous material by PXRD.

(a) Form I, (b) Form I + GM, (c) Form I + LW, (d) Form I + TR-FB, (e) Form I + Myristic acid, (f) Form I + Stearic acid, (g) Form I + Palmitic acid, (h) Form I + Palmitic anhydride, (i) Form I + Stearic anhydride, (j) Form I + Gelucire43/01, (k) Form I + Lauric acid. Blue triangle: Form I (%), Red diamond: Form II (%), Green dotted line: 100-(form I + form II) (%).

Fig. 4 Effects of saturated fatty acid on the phase transition temperature and phase transition rate of CAM form I.

(a) Phase transition temperature, Blue square: T_1 , Red circle: T_2 . (b) Phase transition rate, Blue square: a_1 , Red circle: a_2 . Lau: Lauric acid, Myr: Myristic acid, Pal: Palmitic acid, Ste: Stearic acid.

Fig. 5 Differences between solubility parameter of CAM and saturated fatty acid. Lau: Lauric acid, Myr: Myristic acid, Pal: Palmitic acid, Ste: Stearic acid.

Fig. 6 Effects of the percentage of additive agent on the phase transition temperature and transition rate. (a) Phase transition temperature of Form I + GM, Blue square: T_1 , Red circle: T_2 . (b) Phase transition rate of Form I + GM, Blue square: a_1 , Red circle: a_2 . (c) Phase transition temperature of Form I + Stearic acid, Blue square: T_1 , Red circle: T_2 . (d) Phase transition rate of Form I + Stearic acid, Blue square: a_1 , Red circle: a_2 .

Fig. 7 Effects of additive amounts on the phase transition. (a) Form I + GM (5%), (b) Form I + GM (50%), (c) Form I + Stearic acid (5%), (d) Form I + Stearic acid (50%). Blue triangle: Form I (%), Red diamond: Form II (%), Green dotted line: 100-(form I + form II) (%).

Fig. 8 DSC thermograms of metastable crystals and the additive mixture. (a) Nifedipine form B, (b) Carbamazepine form III.

Fig. 9 Crystal forms of carbamazepine form III and form III/GM or stearic acid mixture.

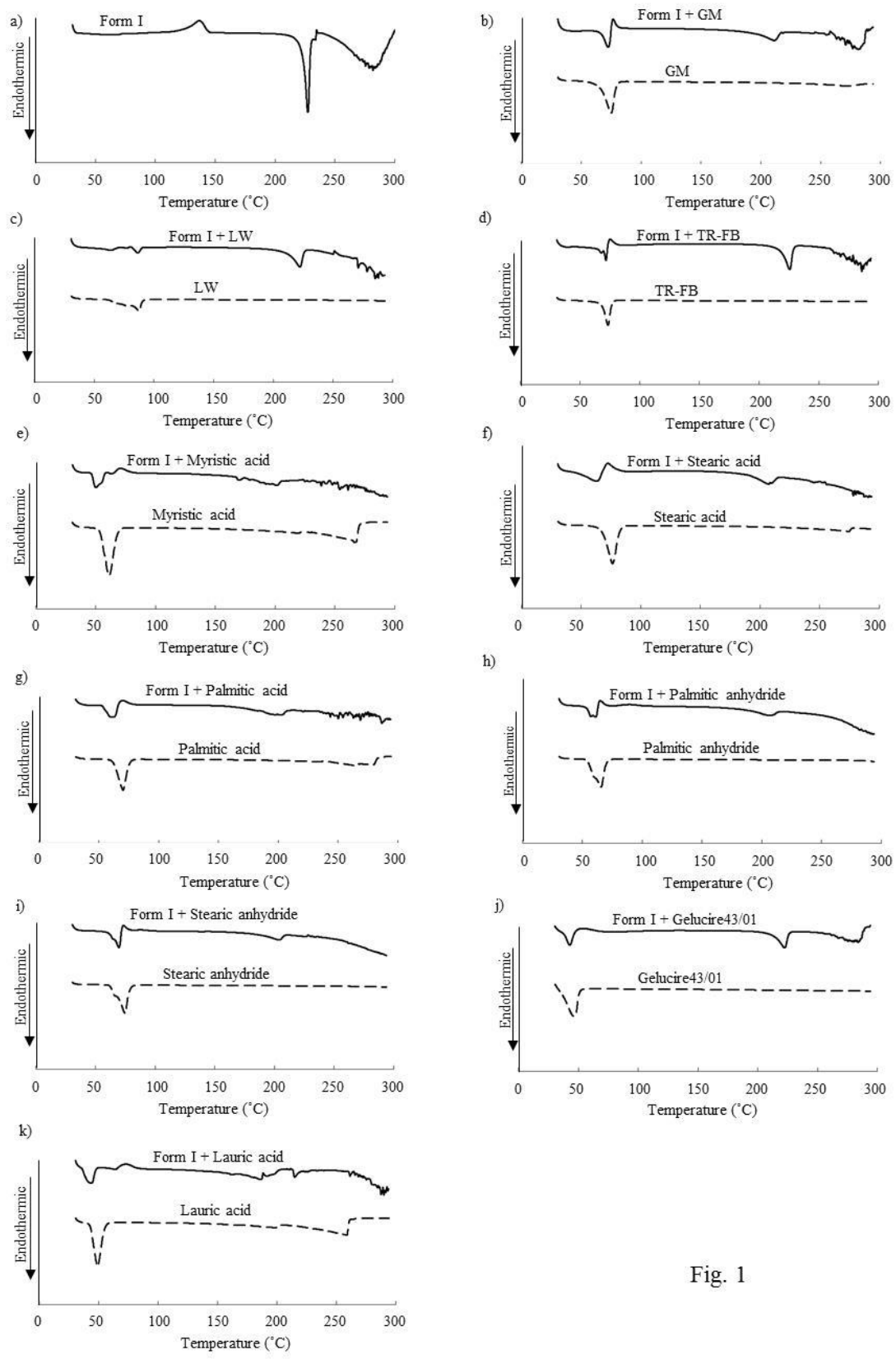


Fig. 1

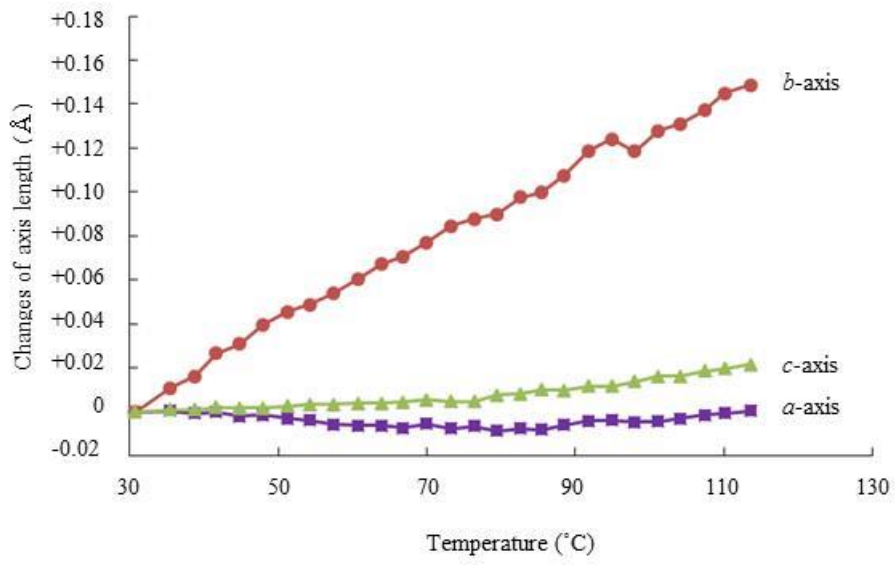


Fig. 2

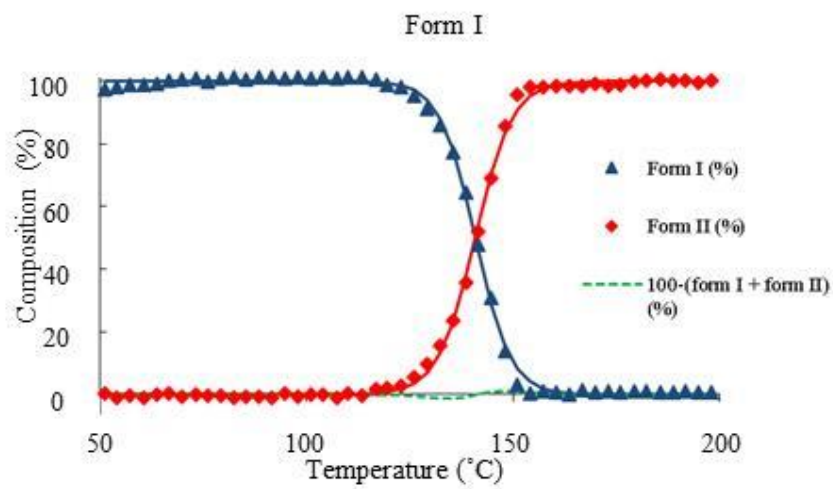
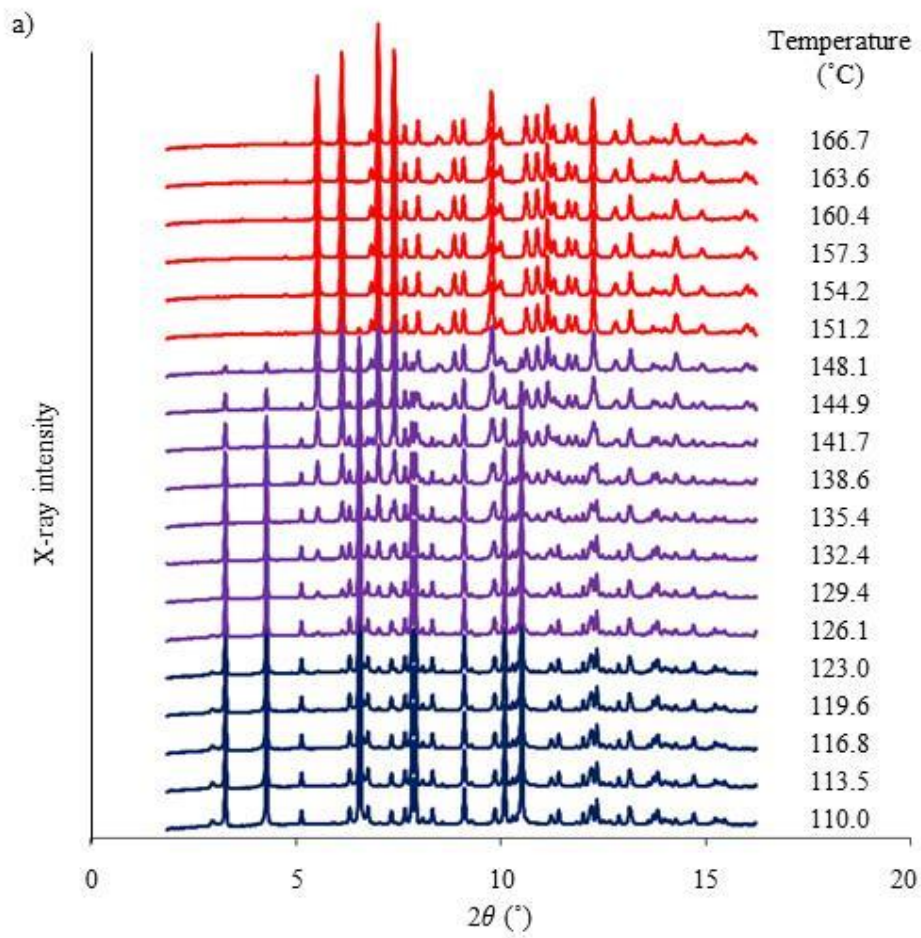


Fig. 3

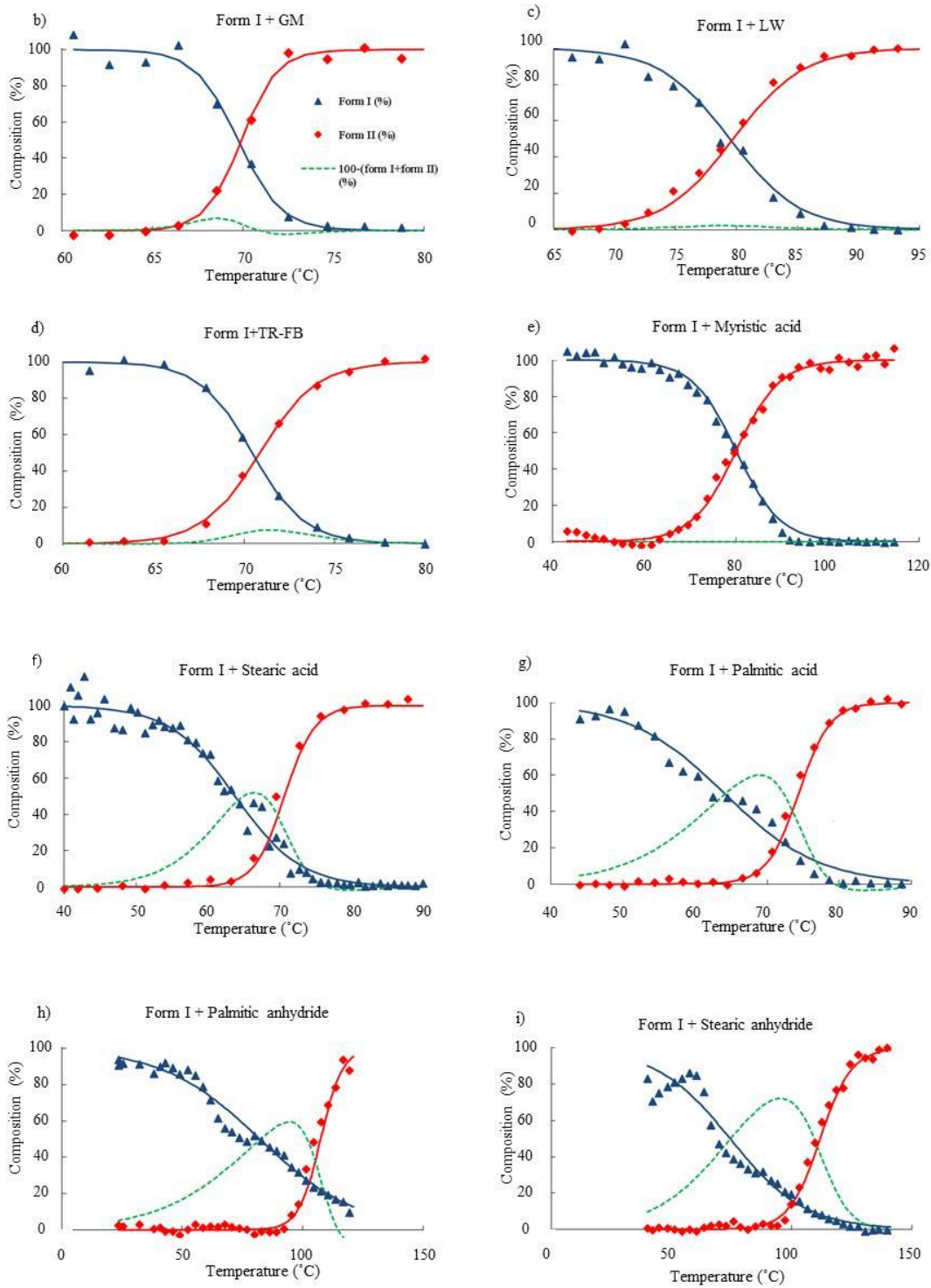


Fig. 3 (continued)

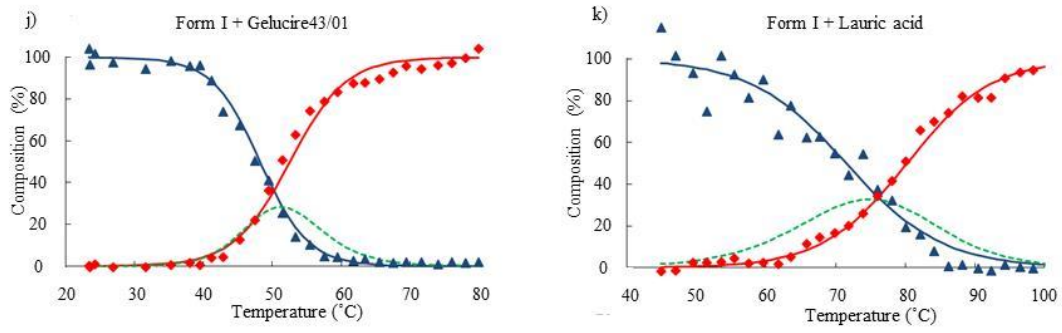


Fig. 3 (continued)

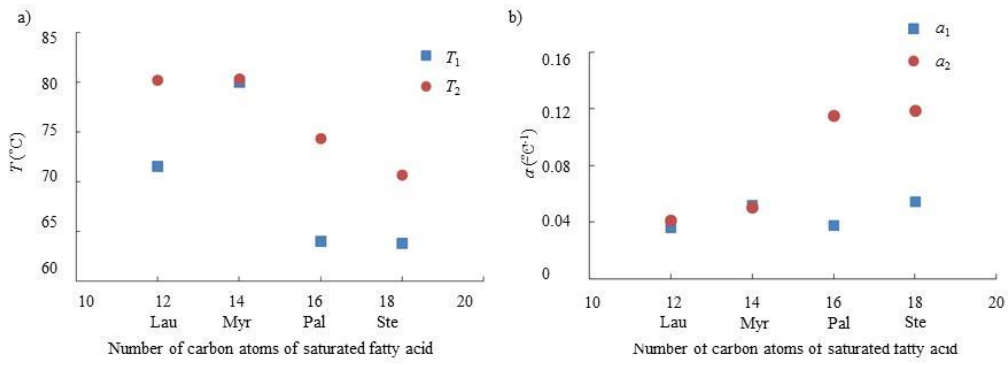


Fig. 4

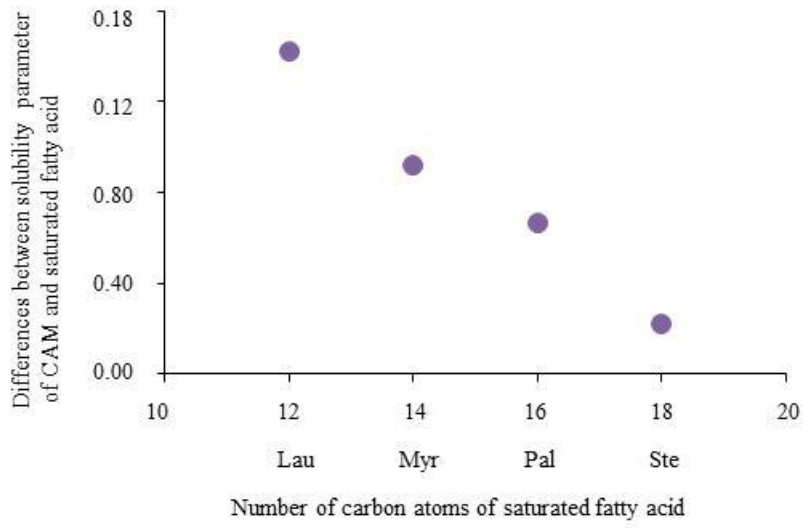


Fig. 5

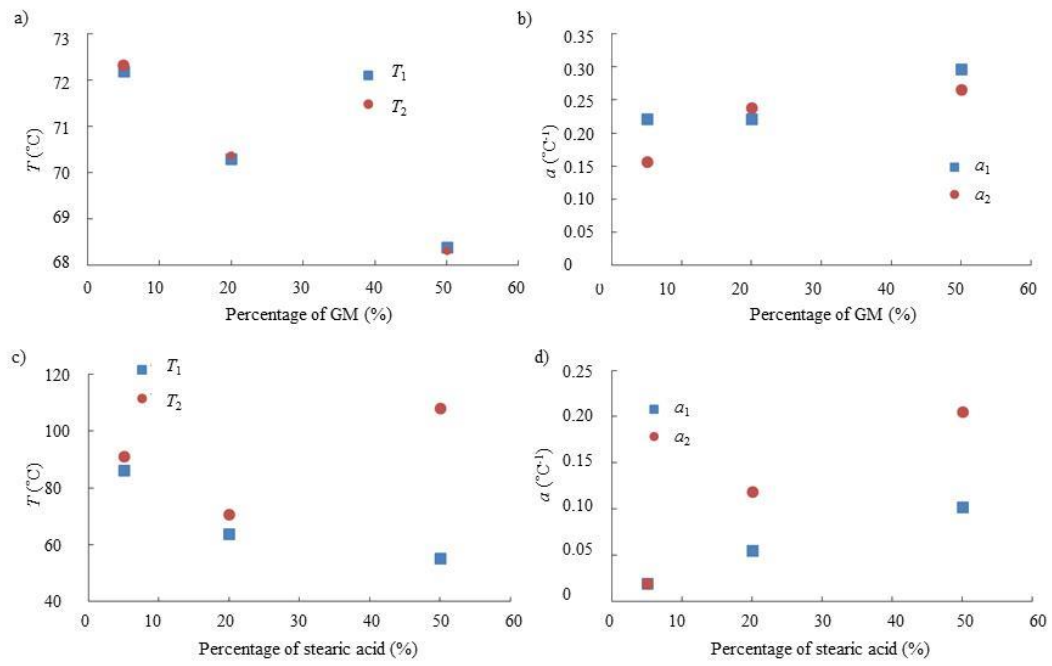


Fig. 6

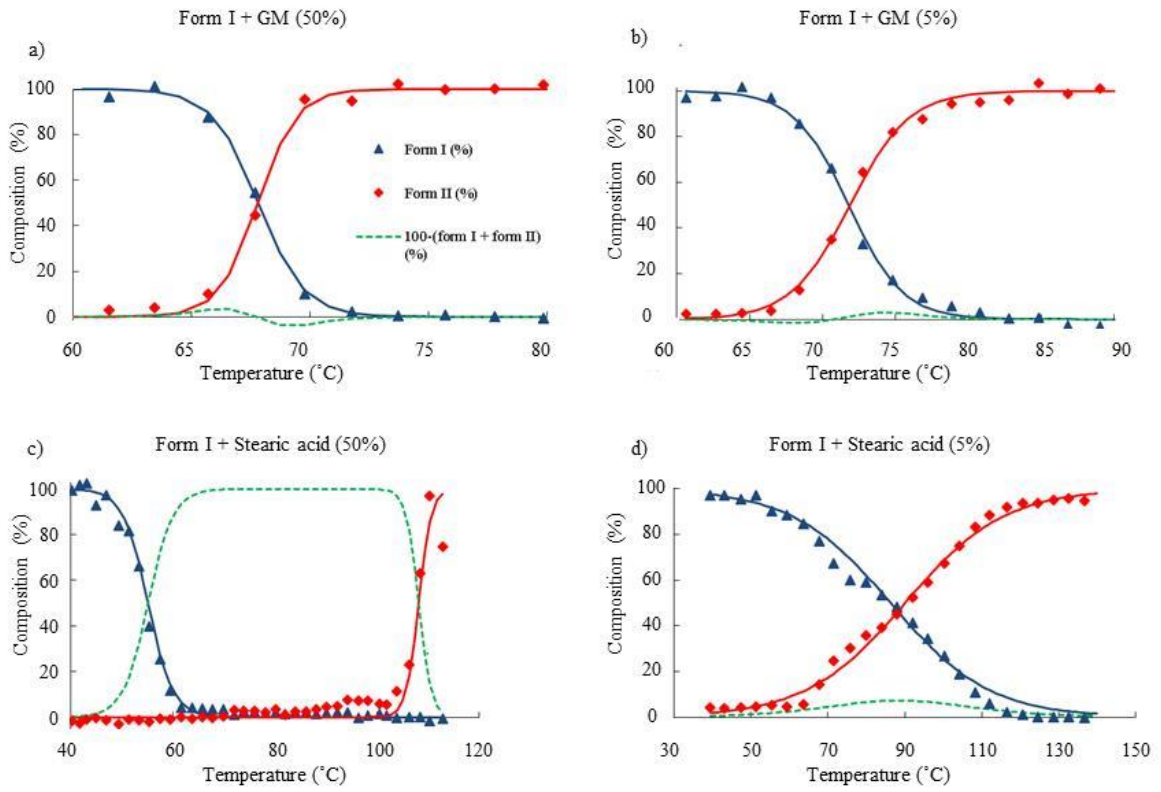


Fig. 7

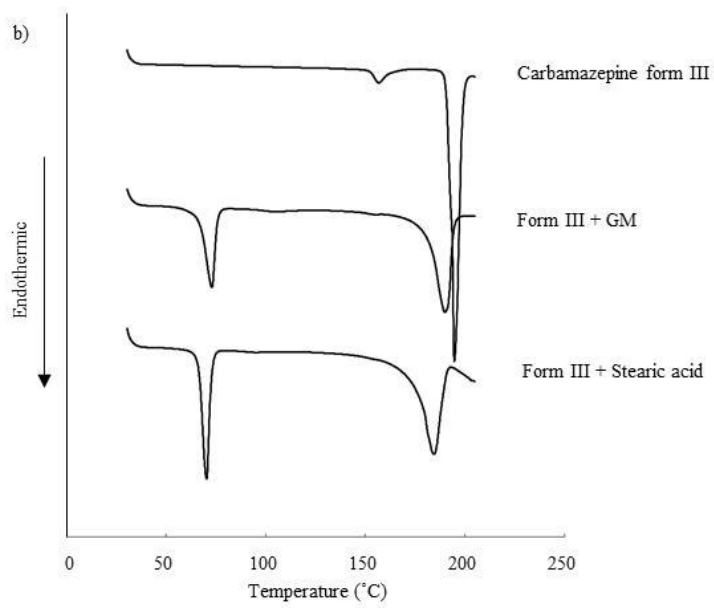
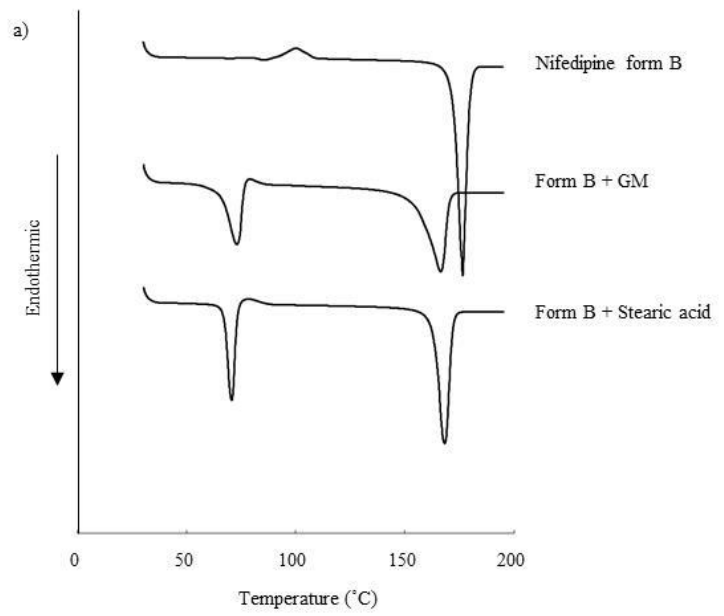


Fig. 8

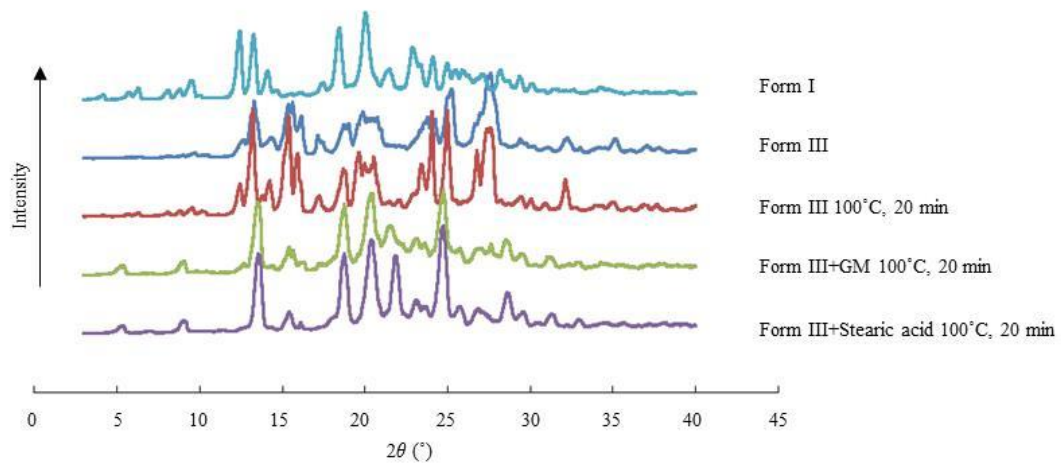


Fig. 9